

Charm in nuclear reactions at $\sqrt{s} = 17$ and 19 GeV¹

Sonja Kabana

Laboratory for High Energy Physics, University of Bern,
 Sidlerstrasse 5, 3012 Bern, Switzerland
 E-mail: sonja.kabana@cern.ch

Abstract

Consequences resulting from the $D\bar{D}$ excess derived indirectly by the NA50 experiment in S+U and Pb+Pb collisions at $\sqrt{s}=19, 17$ GeV, relevant for the identification of the QCD phase transition in these collisions, are discussed. The dependence of open and closed charm yields in Pb+Pb collisions on the number of participating nucleons (N) indicates non thermal charm production and J/Ψ dissociation, stronger than the absorption seen in any other elementary hadron. The J/Ψ in central Pb+Pb collisions could originate dominantly from $c\bar{c}$ pair coalescence out of a hadronizing quark and gluon environment. Furthermore, the J/Ψ appears to be suppressed in S+U collisions at $\sqrt{s}=19$ GeV, as opposed to current interpretations. A significant change in the $(J/\Psi)/D\bar{D}$ ratio as well as in the number density of kaons is observed above energy density $\epsilon \sim 1$ GeV/fm³, suggesting a change of phase at this energy density, and underlining the importance of direct open charm measurements.

1. Introduction

Quantum chromodynamics (QCD) on the lattice predicts a phase transition of confined hadronic matter into deconfined quark and gluon matter (called the Quark Gluon Plasma state – QGP) at a critical temperature $T_c \sim 150$ MeV, respectively at energy density $\epsilon_c \sim 1$ GeV/fm³ [1]. The order of the transition is parameter dependent [2]. An investigation of relevant observables in heavy ion collisions [3] as a function of energy and/or the impact parameter² of the collision could reveal this transition, through a discontinuous behaviour of many QGP signatures at the transition point.

An anomalous suppression of the J/Ψ meson predicted to be a signature of Quark Gluon Plasma formation [4] has been measured to occur in the ratio of the J/Ψ over the Drell Yan (DY) process in Pb+Pb collisions at $\sqrt{s}=17$ GeV investigated as a function of transverse

¹Work supported by the Swiss National Science Foundation.

²Provided that there is a unique assignment between impact parameter and QGP phase transition.

energy (E_T) [5]. In S+U collisions at $\sqrt{s}=19$ GeV and in the most peripheral Pb+Pb collisions, the $(J/\Psi)/DY$ ratio agrees with expectations [5]. The ratio $(J/\Psi)/DY$ is relevant for the investigation of the J/Ψ suppression, under the assumption that J/Ψ production in these collisions is a hard process.

Recent measurements of the dimuon invariant mass $m(\mu^+\mu^-)$ spectrum between the ϕ and the J/Ψ mass (Intermediate Mass Region=IMR) revealed a dimuon enhancement above expectation, which is increasing with the number of nucleons participating in the collision (N) [6]. This enhancement can be understood as due to an excess of $D\bar{D}$ production³ as suggested by several features of the data, e.g. the shape of the mass, rapidity, angular and transverse momentum distributions of the dimuons [6]. The interpretation of the IMR enhancement as due to open charm is not unique though, because the open charm was extracted through a fit to the dimuon continuum and the $D\bar{D}$ meson signal was not directly identified. Recent work suggesting that the seen enhancement could be due to rescattering of D mesons in nuclear matter [7] is not supported by the data [8]. An other possible interpretation is that the IMR excess could be due to thermal dimuons [9]. Non-perturbative effects are known to play a role in heavy flavour hadron production in elementary reactions showing up in deviations of data from perturbative QCD calculations [10,11]. Based on this fact, one could expect that theoretical investigation of non-perturbative effects and different reaction dynamics as in the plasma phase may result in an enhancement of open charm production in nuclear reactions over perturbative QCD expectations.

If the total charm produced in heavy ion collisions indeed deviates from the perturbative QCD expectations for a hard process as suggested by the NA50 data, it follows that the $(J/\Psi)/DY$ ratio is not the proper quantity for the search for the J/Ψ suppression as signature of Quark Gluon Plasma formation in nuclear reactions. It is only the ratio $(J/\Psi)/(\text{total } c\bar{c})$ that matters. We therefore investigate here first the dependence of the J/Ψ and the $D\bar{D}$ yields per collision on N. We further investigate the dependence of the $(J/\Psi)/D\bar{D}$ ratio on N and on the length of the nuclear matter traversed by the J/Ψ , as well as the dependence of both charm and strangeness production on the initial energy density reached in the collision.

2. N dependence of open and closed charm yields in Pb+Pb collisions at $\sqrt{s}=17$ GeV

2.1. N dependence of the Drell Yan yield

Calculation details

The dependence of the Drell Yan (DY) yield per nucleus-nucleus collision in arbitrary units produced in Pb+Pb collisions at $\sqrt{s}=17$ GeV per N+N collision, on the transverse energy of the collision has been measured by the NA50 collaboration (figure 7 in [12]). In this figure it is shown that the theoretically expected DY yield, assuming DY production is

³With ' $D\bar{D}$ ' we denote the number of D and \bar{D} hadrons which were simultaneously found within the acceptance of the NA50 experiment ($D\bar{D} = (D + \bar{D})_{acc}/2$).

a hard process, does partly reproduce the measured one; the deviations at low transverse energy are understood to result from properties of the lead (Pb) nucleus, in particular from the different radii of the proton and neutron distributions in Pb [13]. It is therefore justified to use the theoretically calculated E_T dependence of DY yield per collision, to estimate the dependence of J/Ψ and $D\bar{D}$ yields on the number of participating nucleons in the collision.

However, since the deviations of the very low statistics measurement of DY yield at high E_T , from the theoretical estimated DY yield seen in figure 7 of [12] cannot be understood, it would be important to *measure* the DY yield per collision with high statistics in the high E_T region. In this way the last drop in the $(J/\Psi)/DY$ ratio above $N \sim 360$ [5] can be experimentally verified.

2.2. N dependence of the $D\bar{D}$ yield

Calculation details

The NA50 collaboration observed an excess (E) of the measured over the expected $D\bar{D}/DY$ ratio in S+U and Pb+Pb collisions at $\sqrt{s}=19, 17$ GeV, which increases with the number of participants N (figure 12 and table 4 in [6]). If we fit the S+U and Pb+Pb E points of the above figure to a function $f = c \cdot N^\alpha$, we find that the excess is increasing with N as $N^{(\alpha=0.45\pm 0.11)}$ ($\chi^2/\text{Degrees Of Freedom}=1.7$, DOF=7). The N dependence of the excess E of the $D\bar{D}/DY$ production in S+U collisions at $\sqrt{s}=19$ GeV and Pb+Pb collisions at $\sqrt{s}=17$ GeV over expectations, reflects the N dependence of the $D\bar{D}/DY$ ratio. This results from the fact, that all other quantities involved in the definition of E [6,8], do not depend on N. Therefore the N dependence of the $D\bar{D}$ production yield is given by the N dependence of the quantity

$$n_{D\bar{D}} = E * n_{DY} \sim (D\bar{D}/DY) * n_{DY} \quad (1)$$

where $n_{D\bar{D}}$, n_{DY} denote the yields of $D\bar{D}$ and DY per collision in arbitrary units. The arbitrary units are due to the fact that NA50 did not published absolute yields per collision of the J/Ψ , DY and $D\bar{D}$ separately, corrected for losses due to e.g. acceptance, as a function of N, E_T . We suggest that it would be important to do so.

The DY yield used for the above calculation has been extracted from the theoretical curve shown in figure 7 in [12], at the transverse energy (E_T) points in which the $D\bar{D}$ excess factor E has been measured. The E_T points corresponding to the excess factor E were extracted, by interpolating between the E_T values given in table 1 of [12] as a function of the mean impact parameter, at the values of mean impact parameter for which the factor E has been measured (listed in table 1 of [6]). For the most central and the most peripheral points, for which no mean b are given in table 1 of [6], we estimated the values of b, from the values of N as a function of b for Pb+Pb collisions calculated by [14,15]. These calculations [14] agree with the values (N,b) estimated by NA50, when compared

in their common range.

Though the $D\bar{D}$ measured by NA50 represents the joint probability that a D and a \bar{D} are both found in the experimental acceptance, the N dependence of it, is expected to be the same or similar to the N dependence of the sum $D + \bar{D}$, respectively of the D , and of the \bar{D} hadrons. It is however possible that the above N -dependences deviate from each other, in case of a higher than 1 charm pair multiplicity per event with charm (see [16] for a numerical estimation of the charm multiplicity per event in central Pb+Pb collisions at 158 A GeV). Therefore, for clarity, the N dependence of the total extrapolated $D + \bar{D}$ yield in nuclear collisions should be estimated including acceptance corrections by NA50.

Results and discussion

The resulting $D\bar{D}$ yield in arbitrary units (figure 1) increases as $N^{(\alpha=1.70\pm 0.12)}$ ($\chi^2/DOF = 2.5$, $DOF=7$). This N behaviour indicates that $D\bar{D}$ production in Pb+Pb collisions at $\sqrt{s}=17$ GeV, did not establish yet equilibrium, in which case a proportionality with N –assuming N to be proportional to the volume of the source⁴– is expected ($\alpha=1$). This appears justified because the temperature in the collision zone –assuming local thermalization of light particles– drops with time and the mean temperature expected to be reached in these collisions of the order $\sim 10^2$ MeV, is much lower than the mass of charm quarks and/or charmed hadrons.

2.3. N dependence of the J/Ψ yield

Calculation details

In the following we estimate the J/Ψ yield per collision as a function of N , at the same N values where the $D\bar{D}$ was measured. The N dependence of the J/Ψ yield per collision is given by the N dependence of the quantity :

$$n_{J/\Psi} = ((J/\Psi)/DY) * n_{DY} \quad (2)$$

where $n_{J/\Psi}$, n_{DY} denote the yields of J/Ψ and DY in arbitrary common units. The $(J/\Psi)/DY$ values have been extracted from figure 4 of [5] at the E_T values where the E factor has been measured, interpolating between the different points.

Results and discussion

The resulting J/Ψ yield per collision produced in Pb+Pb collisions in arbitrary units (figure 2) increases like $N^{(\alpha=0.70\pm 0.04)}$ ($\chi^2/DOF=1.43$, $DOF=7$). This N dependence indicates an increasing J/Ψ dissociation with higher centrality. The strength of this dissociation as measured by the α parameter, is higher for the J/Ψ as compared to any other hadron⁵

⁴ The assumption $N \sim V$, is based on the observation that the freeze out volume V of the particle source is found to be proportional to N [17].

⁵ Deuterons have an even smaller α parameter, but they are not elementary hadrons and are weakly bound (see discussion in [17]).

produced in these collisions for example as compared to antiprotons. For the latter, a large annihilation cross section with baryons is expected and there is indeed experimental evidence that they are absorbed with increasing centrality in Pb+Pb collisions ($\alpha(\bar{p})=0.80 \pm 0.04$, ($\chi^2/DOF=1.0$, $DOF=3$) at $y=3.7$, $p_T=0$ [17]⁶).

The J/Ψ multiplicity as a function of N extracted with an other method [18], agrees with the here presented results within the errors.

3. The $(J/\Psi)/D\bar{D}$ ratio in nuclear collisions

3.1. The N dependence of the $(J/\Psi)/D\bar{D}$ ratio in nuclear collisions

Calculation details

Assuming that the IMR excess is due partly or solely to open charm, allows us to search for an anomalous suppression of J/Ψ as compared to the open charm production. The N dependence of the $(J/\Psi)/D\bar{D}$ ratio in Pb+Pb and S+U collisions at \sqrt{s} of 17 and 19 GeV, estimated as:

$$(J/\Psi)/D\bar{D} \sim ((J/\Psi)/DY)/(D\bar{D}/DY) \sim ((J/\Psi)/DY)/E \quad (3)$$

in arbitrary units due to the E factor in equation (3), is a decreasing function of N (figure 3). The $(J/\Psi)/DY$ in S+U collisions was taken from [19,20]. Note that possible deviations of the DY yield from its theoretical calculation (as seen in figure 7 in [12]), do not drop out in the $((J/\Psi)/DY)/(D\bar{D}/DY)$ ratio shown here, because the $D\bar{D}/DY$ –unlike the $(J/\Psi)/DY$ – was calculated by NA50 not using the minimum bias theoretical DY yield values but the measured ones.

In order to show the influence of the very last drop of $(J/\Psi)/DY$, on the $(J/\Psi)/D\bar{D}$ ratio, the $(J/\Psi)/DY$ ratio divided by $N^{0.45 \pm 0.11}$ is plotted as a function of N in figure 4. This quantity resembles the $(J/\Psi)/D\bar{D}$ ratio

$$(J/\Psi)/D\bar{D} \sim ((J/\Psi)/DY)/N^{0.45 \pm 0.11} \quad (4)$$

in arbitrary units, because $N^{0.45 \pm 0.11}$ is the found N dependence of the $D\bar{D}/DY$ ratio. The open points of figure 4 are extracted from the 'minimum bias analysis' results of figure 4 in [5]⁷. The closed points show the $((J/\Psi)/DY)/N^{0.45}$ calculated here, at the N values where the $D\bar{D}$ excess factor was measured.

Results and discussion

⁶We extracted here the α parameter for \bar{p} , after quadratically adding the statistical and a 5% systematic error.

⁷'Minimum bias analysis' in NA50, means that the DY for the $(J/\Psi)/DY$ ratio, was determined using the theoretically estimated DY yield per collision as a function of E_T and the measured dN/dE_T vs E_T spectrum of minimum bias trigger events (see [12]).

The $(J/\Psi)/D\bar{D}$ ratio in Pb+Pb collisions found as shown in equation (3), decreases with N as $N^{(\alpha=-0.79\pm 0.14)}$ ($\chi^2/DOF = 3.3$, $DOF=7$), respectively like $N^{(\alpha=-1.17\pm 0.14)}$ ($\chi^2/DOF=1.54$, $DOF=6$) when the first point is not fitted⁸. The $(J/\Psi)/D\bar{D}$ ratio in S+U collisions (figure 3) decreases with N as $N^{(\alpha=-0.62\pm 0.22)}$ ($\chi^2/DOF=0.69$, $DOF=3$). The $(J/\Psi)/D\bar{D}$ found as shown in equation (4) when fitted to the function N^α until $N=380$, gives $N^{(\alpha=-1.07\pm 0.07)}$, ($\chi/DOF=0.93$, $DOF=7$).

If the J/Ψ is completely dissociated in a quark gluon plasma and is formed later mainly through c and \bar{c} quark coalescence, we expect that the N dependence of the ratio $(J/\Psi)/D\bar{D}$ –rather than the $(J/\Psi)/(D\bar{D})^2$ – reflects the N dependence of the volume of the charm environment [10]. This is due to the expectation that because of the very low cross section of charm production at these energies, there is most often just one $c\bar{c}$ pair per event containing charm, whatever N . Then the probability to form a J/Ψ from coalescence is proportional to $(J/\Psi)/D\bar{D}$ and inversely proportional to the volume of the particle source –made up by $u\bar{u}d\bar{d}s\bar{s}$ quarks and gluons– within which the c and \bar{c} quarks scatter. Assuming this volume is proportional to N (see footnote 3), one would expect that $(J/\Psi)/D\bar{D}$ decreases as N^{-1} , as actually observed.

In this case, one can use the $(J/\Psi)/D\bar{D}$ ratio to extract the absolute value of the volume of its environment with a coalescence model. The 'charm' coalescence volume would reflect partly the QGP hot spot volume and partly the hadronic source volume from which hadrons with charm and anticharm can also form a J/Ψ . If the absolute yields per collision of J/Ψ and $D\bar{D}$ as a function of N , needed for this calculation would be published by NA50, the charm coalescence volume could be calculated.

Figure 4 suggests that the coalescence picture could hold for the full N range of Pb+Pb collisions up to $N=380$. Obviously, it would be better to use the $D\bar{D}$ data themselves instead of the N parametrization, if high enough statistics would be available.

On the other hand, if the multiplicity of charm quarks is high enough that often more than 1 charm quark pair per event with charm is produced, then it is the ratio $(J/\Psi)/(D\bar{D})^2$ which is expected to be inversely proportional to the volume of the charm source (this is exactly the case if d coalescence out of p and n is investigated in a baryon rich source). The N dependence of the $(J/\Psi)/(D\bar{D})^2$ ratio, which would be relevant in the above discussed case is $N^{(\alpha=-2.26\pm 0.48)}$, ($\chi^2/DOF=2.5$, $DOF=7$) respectively $N^{(\alpha=-3.1\pm 0.24)}$, ($\chi^2/DOF=1.2$, $DOF=6$) if the first point is not fitted. The question on the absolute multiplicity of charm in nuclear reactions, should be answered by experiment.

3.2. The L dependence of the $(J/\Psi)/D\bar{D}$ ratio in nuclear collisions

Calculation details

⁸The first point of the $D\bar{D}/DY$ enhancement factor E lies significantly above the N^α function fit to the E distribution (figure 12 in [6]).

The two distributions of $(J/\Psi)/D\bar{D}$ ratio for S+U and Pb+Pb collisions in figure 3, are measured at different energies, and therefore they cannot be compared in terms of their absolute yields but only with respect to their shapes. In order to compare their absolute yields, the data from figure 5 of [20] will be used. There the $(J/\Psi)/DY$ ratio in p+A, S+U and Pb+Pb collisions is shown as a function of L, all normalised to the same energy ($\sqrt{s}=19$ GeV) and corrected for the isospin dependence of DY production. The parameter L, is the length that the J/Ψ traverses through nuclear matter. In order to convert figure 5 of [20] to the $(J/\Psi)/D\bar{D}$ ratio as a function of the L parameter, the $(J/\Psi)/DY$ ratio data points have been divided by the E factor as described in equation (3). The correlation of the L parameter with N and b for Pb+Pb collisions, has been estimated using the theoretical calculation of [14].

Results and discussion

The L dependence of the $(J/\Psi)/D\bar{D}$ ratio in arbitrary units in p+A, S+U and Pb+Pb collisions calculated here, is shown in figure 5, together with the $(J/\Psi)/DY$ ratio published in [19,20]. The closed points show the $(J/\Psi)/D\bar{D}$ ratio in S+U and Pb+Pb collisions extracted as indicated in equation 3. The open squares and circles show the $(J/\Psi)/DY$ ratio in S+U and Pb+Pb collisions from [19,20]. The open stars, show both the L dependence of the $(J/\Psi)/DY$ as well as the L dependence of the $(J/\Psi)/D\bar{D}$ in p+A collisions which are the same, since the factor E has the value 1 for the latter.

The J/Ψ over the $D\bar{D}$ production investigated as a function of the volume through which the J/Ψ traverses ($V \sim L^3$) is suppressed as compared to the shape of the exponential fit going through the $(J/\Psi)/D\bar{D}$ p+A data, in both the S+U and Pb+Pb collisions at all L points (figure 5).

The energy density of the lowest S+U point has been estimated to be ~ 1.1 GeV/fm³ [5], which is comparable to the predicted critical energy density for the QGP phase transition of ~ 1 GeV/fm³. A similar energy density of 1.2 GeV/fm³ has been estimated [5] to be reached in the most peripheral Pb+Pb collisions measured by NA50.

In the following we investigate the initial energy density, rather than only the volume of the particle source ($V \sim L^3$), as a critical parameter for the appearance of the QGP phase transition.

4. The ϵ dependence of charm and strangeness in nuclear collisions

4.1. Charm

Calculation details

We estimate here the $(J/\Psi)/D\bar{D}$ ratio as a function of the energy density ϵ . For this purpose we use part of the data shown in figure 7 in [5]. There the ratio of $((J/\Psi)/DY)_{measured}$ over the $((J/\Psi)/DY)_{expected}$ is shown. The ' $((J/\Psi)/DY)_{expected}$ ', is taken to be the exponential fit seen in figure 5, which represents the 'normal' J/Ψ dissociation (i.e. understood without invoking QGP formation). Dividing these data points by $N^{0.45\pm 0.11}$, and normalising the distribution of S+U and Pb+Pb points to the p+p and p+A data as in figure 5, we estimate the $((J/\Psi)/D\bar{D})$ ratio over the expectation expressed by the above mentioned exponential curve, which fits the $((J/\Psi)/D\bar{D})$ data points for p+p, p+d and p+A collisions.

Results and discussion

The result of this calculation is shown in figure 6 in logarithmic scale and in figure 7 (a) in linear scale. It demonstrates a deviation of the $(J/\Psi)/D\bar{D}$ ratio both in S+U and Pb+Pb collisions, from the p+p and p+A expectation curve, occurring above $\epsilon \sim 1 \text{ GeV}/\text{fm}^3$. The logarithmic scale is shown to reveal small changes in the slope of the $((J/\Psi)/D\bar{D})$ distribution as a function of ϵ , appearing at $\epsilon \sim 2.2$ and $3.2 \text{ GeV}/\text{fm}^3$.

4.2. Strangeness

Figure 7 compares the two QGP signatures of J/Ψ suppression and of strangeness enhancement. For this purpose we represent all data points as a function of the estimated energy density. Note that the energy density as critical scale variable, has the advantage that unlike the temperature, it is defined irrespective of whether equilibrium is reached in the collisions studied.

Figure 7 (b) shows the multiplicity of kaons per event (K^+ , but also some K_s^0 data scaled to K^+ are shown) divided by the effective volume of the particle source at thermal freeze out in the center of mass frame, as a function of the initial energy density. The effective volume represents the part of the real source volume, within which pions are correlated with each other (the so called 'homogeneity' volume in the literature [21]). The effective volume is smaller than but proportional to the real source volume. For a more precise calculation of the freeze out source volume a detailed model is needed. Here we estimate the effective volume at thermal freeze out $V_{thermal}$ based on measurements. The (smaller) effective volume at chemical freeze out $V_{chemical}$, is not experimentally measured, we give however an estimate of the ratio $V_{chemical}/V_{thermal}$. Note that we compare the kaon data without rescaling for the different energy between AGS and SPS⁹.

Calculation details

The effective volume V of the particle source has been estimated in the center of mass

⁹ The total K^+ multiplicity in p+p collisions, increases by a factor of ~ 5 , from 11.1 to 158 GeV per nucleon [22].

frame, assuming cylindrical shape of the source:

$$V = (\pi \cdot Radius_{cylinder}^2) \cdot Length_{cylinder} \rightarrow$$

$$V = (\pi \cdot 4 \cdot R_{side}^2) \cdot (\sqrt{12} \cdot R_{long})$$

where R_{side} is a measure of the transverse radius and R_{long} is a measure of the longitudinal radius of the particle source, and the factors 4 and $\sqrt{12}$ arise from the definition of R_{side} , R_{long} [21]. The R_{side} and R_{long} values for central Au+Au collisions at 10.8 A GeV and for central Pb+Pb collisions at 158 A GeV have been taken from [23]. We dont use the more elaborated estimation of the homogeneity volume given in [24], because the R_{ol} component is not given in [23]. Based on the data of [23] we estimated the effective volume of the source at thermal freeze out in central Au+Au collisions at 10.8 A GeV ($V \sim 1949 fm^3$) and central Pb+Pb collisions at 158 A GeV ($V \sim 6532 fm^3$). The effective volume increases by a factor of 3.35 from AGS to SPS energy.

Based on the temperature at thermal and chemical freeze out which has been estimated from measurements using thermal models [25], and the above estimated volumes at thermal freeze out, we can further estimate the volume at chemical freeze out. For this we assume that the relation $V \sim T^{-3}$, which holds in the universe for massless particles in thermal equilibrium and for adiabatic expansion [26], holds approximately for heavy ion collisions at AGS and SPS energy. Then from the temperature values at thermal and chemical freeze out given in [25] averaged over all models, we find that the ratio $V_{chemical}/V_{thermal}$ (AGS Si+Au 14.6 A GeV) =0.45 and $V_{chemical}/V_{thermal}$ (SPS Pb+Pb 158 A GeV) = 0.28. Using the volume at chemical freeze out as estimated above, would stretch the K/V ratio in figure 7 (b) between SPS and AGS, by a factor ~ 1.6 apart. We dont use these values in figure 7, because the above calculation is model dependent, e.g. the assumption of massless particles is not met, while the assumption of thermal equilibrium may not be true.

The ratio K/N is expected to be proportional to the number density of kaons $\sim K/V$, (V =volume), assuming $V \sim N$ (for justification of this assumption see footnote 3, [23] and [27]). Based on this expectation, we estimated here the K/V ratios from the K/N ratios, by normalising the K/N ratios to the K/V value of the most central Au+Au events of E866 respectively Pb+Pb events of NA49, for which the value of the volume has been estimated above.

The kaon data from Au+Au collisions at 11.1 A GeV (E866 and E802 experiments) [28] and from Pb+Pb collisions at 158 A GeV (NA49 experiment) [29] are kaon multiplicities extrapolated to full acceptance. Therefore NA49 and E866 data are absolutely normalised. We estimated K/N from the NA49 experiment using the kaon multiplicities from [29] and the number of wounded nucleons from [30] as available¹⁰, otherwise we used the N estimated from the experimental baryon distribution [29].

¹⁰ We take N equal to the number of wounded nucleons for NA49, because it is used in all other experiments presented here, and allows for a straightforward geometrical interpretation of N .

The data from NA52 [17] and WA97 [31] have been measured in a small phase space acceptance and have been scaled here arbitrarily, in order to match the NA49 data in figure 7. This scaling is justified since all NA52, NA49 and WA97 measurements are kaons produced in Pb+Pb collisions at 158 A GeV, and 'extrapolates' the NA52 and WA97 data to the NA49 full acceptance multiplicities, allowing for comparison of the shapes of the distributions. It is assumed, that the N and ϵ dependence of kaons does not change significantly with the phase space acceptance.

In order to calculate the energy density we have performed the following steps. The energy density for all colliding systems has been estimated using the Bjorken formula [32] and data given in [28,33,34]. The transverse radius of the overlapping region of the colliding nuclei is found as: $R_{trans} = 1.13 \cdot (N/2)^{1/3}$, where N is the total number of participant nucleons. The formation time was taken 1 fm/c [32].

For the E866 experiment, lacking E_T values, (but with measured $E_{forward}$), we used instead of $(dE_T/d\eta)_{y_{cm}}$, (y_{cm} =midrapidity) the total energy of the nucleons participating in the collision ($E_{tot,part} = N_{projectile,participants} \cdot E_{beam}$), assuming the proportionality $(dE_T/d\eta)_{y_{cm}} \sim E_{tot,part}$, and we further normalised the results in such a way that the maximum energy density of our estimate matches the absolute value of the maximal achieved energy density in the most central Au+Au events at this energy of 1.3 GeV/fm³, given in [33].

NA52 measures E_T near midrapidity ($y \sim 3.3$). These values were used to estimate the energy density and the results have been normalised to the maximum energy density reached in Pb+Pb collisions at the same centrality of $\epsilon_{max}=3.2$ GeV/fm³, extracted by NA49 in [34]. Parametrizing the dependence of the energy density on the number of participants found from the NA52 data as described above, we estimated the energy density corresponding to the N values of the WA97 and the NA49 kaon measurements, given in [31,29]. Data from S+S collisions taken from [29] and [35,34] are also shown.

To estimate the systematic error on the energy density found with the above methods, we calculated the energy density in Pb+Pb collisions at 158 A GeV, using the VENUS 4.12 [36] event generator. We estimated with VENUS the $(dE_T/d\eta)_{y_{cm}}$ at y_{cm} =midrapidity and the number of participant nucleons and used them to find the energy density from the Bjorken formula [32]. The deviation of the energy density calculated with VENUS $(dE_T/d\eta)_{y_{cm}}$ from the energy density found using the NA52 transverse energy measurements is $\leq 30\%$ of the latter. The deviation of the energy density calculated with VENUS $dE_T/d\eta$ from the energy density found using the total energy of the participant nucleons and of the newly produced particles, (which is similar to the method used to estimate the energy density for the AGS data), over the latter energy density, is at the same level.

In this context, it appears important for a more precise comparison of data as a function of ϵ , that experiments publish together with the number of participants also the $dE_T/d\eta$ at midrapidity for each centrality region, for both nucleus+nucleus and for p+p collisions,

estimated by models or measured if available (e.g. in NA49).

Results and discussion

Figure 7 (b) suggests that kaons below $\epsilon \sim 1 \text{ GeV/fm}^3$ did not reach equilibrium, while this seems to be the case above. Indeed kaons produced in Au+Au collisions at 11.1 A GeV [28] and in very peripheral Pb+Pb collisions at 158 A GeV [37,38,17], increase faster than linear with N, indicating non thermal kaon production, while they increase nearly proportional to N above $\epsilon \sim 1 \text{ GeV/fm}^3$ [38,17,31]. The connection of strangeness equilibrium and the QGP phase transition has been discussed e.g. in [39]. There it is shown, that strangeness in heavy ion collisions is expected to reach equilibrium values if the system runs through a QGP phase, while this is less probable in a purely hadronic system.

Figure 7 demonstrates that both the J/Ψ and kaon production exhibit a dramatic change above the energy density of $\sim 1 \text{ GeV/fm}^3$. While the equilibration of strange particles as suggested by their $\sim N^1$ dependence above 1 GeV/fm^3 , could in principle also be due to equilibrium reached in a hadronic environment, the combined appearance of this effect and of the $(J/\Psi)/D\bar{D}$ suppression at the same energy density value is a striking result, indicating a change of phase above $\epsilon_c=1 \text{ GeV/fm}^3$.

The expectation for the shape of the J/Ψ suppression as a function of energy density are three successive drops of the J/Ψ [40,5]; a drop by $\sim 8\%$ [18] due to ψ' dissociation, a drop by $\sim 32\%$ [18] due to the χ_c dissociation and a drop by $\sim 100\%$ due to the J/Ψ dissociation. All these without taking into account regeneration of J/Ψ through other processes. These can be e.g. coalescence of charm quarks or J/Ψ not travelling through the plasma. The ψ' feeds only 8% of the total J/Ψ 's and can therefore hardly be observed as a break in the J/Ψ production.

The absolute value of the energy density ϵ and therefore of the N values at which these changes could be observed is not exactly given by the models. The critical energy densities for the dissociation of the states Ψ' , χ_c and J/Ψ could even be so near to each other that no clear multistep behaviour is seen in $(J/\Psi)/D\bar{D}$.

Figure 7 suggests that the breaks in the $(J/\Psi)/D\bar{D}$ ratio at $\epsilon \sim 2.2$ and 3.2 GeV/fm^3 , are less dramatic than the change above $\epsilon \sim 1 \text{ GeV/fm}^3$. Therefore, all bound $c\bar{c}$ states could be dissociated at similar energy densities, which lie near 1 GeV/fm^3 .

Alternatively, the ψ' and the χ_c could dissociate above $\epsilon \sim 1 \text{ GeV/fm}^3$ and the dissociation of the J/Ψ could start at $\epsilon=2.2 \text{ GeV/fm}^3$, if we interpret the change in the $(J/\Psi)/D\bar{D}$ ratio, below and above $\epsilon=2.2 \text{ GeV/fm}^3$, as a step behaviour. In this context, the steep drop of the $(J/\Psi)/D\bar{D}$ ratio in the bin(s) of largest N (figures 4, 6, 7), cannot be interpreted in a natural way. The steps of $(J/\Psi)/D\bar{D}$ remain to be established through a direct measurement of J/Ψ and $D\bar{D}$ absolute yields as a function of (E_T, N, ϵ) .

In the above discussed picture, three QGP signatures appear in nuclear collisions at energy density larger than $\sim 1 \text{ GeV}/\text{fm}^3$:

- a) J/Ψ suppression (figure 7 (a)) –which could be due to bound $c\bar{c}$ states dissociation–
 - b) strangeness enhancement (figure 7 (b)), possibly due to equilibration of $s\bar{s}$ in QGP as opposed to hadrons,
 - c) the invariant mass $m(e^+e^-)$ excess at m below the ρ mass [41], possibly due to a ρ change [42] and/or to increased production of the lowest mass glueball state in QGP [43].
- This coincidence of QGP signatures, suggests a change of phase at $\epsilon \sim 1 \text{ GeV}/\text{fm}^3$ as expected [1].

From the above discussion it follows, that a direct measurement of open charm production in nuclear collisions appears essential for the physics of the Quark Gluon Plasma phase transition. Furthermore, if enhanced over expectations, open charm in nuclear collisions defies theoretical understanding.

5. Possibilities for future measurements

A measurement of open and closed charm production in Pb+Pb collisions as a function of energy below the SPS top energy of $\sqrt{s} = 17 \text{ GeV}$ searching for the disappearance of the seen J/Ψ suppression in central Pb+Pb collisions at a certain \sqrt{s} , could prove clearly the QGP phase transition. Using the same nuclei at different \sqrt{s} and looking only at central collisions, differences due to different nuclear profiles drop out. No currently existing or planned experiment at SPS is however able to perform this measurement without major upgrades, though one proposal (NA6i) could significantly improve the identification of open charm production through a better determination of the decay vertex [44]. An upgrade of NA50/NA6i, or alternatively a completely new experiment, could possibly achieve this goal. The study could also be performed at the Relativistic Heavy Ion Collider (RHIC) using lower energy and/or large and small nuclei, and in fixed target experiments at RHIC favoured because of higher luminosity as compared to the collider mode, important for a low energy scan.

It would be also important (and easier than the above) to measure the J/Ψ , $D\bar{D}$ and DY absolute yields per collision, below $\epsilon=1 \text{ GeV}/\text{fm}^3$, by using the most peripheral (not yet investigated) Pb+Pb collisions or collisions of lighter nuclei at the highest beam energy at SPS ($\sqrt{s} = 17,19 \text{ GeV}$).

An other piece of information important for the understanding of charm production in nuclear collisions would be the direct comparison of the $(J/\Psi)/DY$ and the $(J/\Psi)/D\bar{D}$ ratios in nuclear collisions at $\sqrt{s} < 19 \text{ GeV}$ and in $p + \bar{p}$ collisions at the Tevatron. Tevatron reaches an energy density similar to or larger than the one estimated in very central S+S collisions at 200 A GeV [45]. Therefore it would supply a comparison for these points and a continuation of the absorption line fitted through the p+p and p+A data measured by NA50 (figure 5), or otherwise. Differences due to the change of dominant production

mechanisms of charm in $p\bar{p}$ collisions as compared to A+B, p+p, can be accounted for theoretically. A high E_T cut could additionally help in sorting out 'central' $p + \bar{p}$ collisions. This comparison should be done possibly in the very same dimuon mass region for all processes (also DY) e.g. using Monte Carlo's tuned to $p + \bar{p}$ Tevatron data.

This comparison would answer the question, if the energy density is indeed the only critical variable for the appearance of a thermalised QGP state with 3 effective flavours u,d,s, or whether there is also a critical volume (e.g. as measured by the L variable: $V \sim L^3$). Furthermore, at present the comparison of nuclear collisions to p+p and p+A data is done at the same energy and not at the same energy density. This issue is important, since if for example the energy density is the only critical scale variable, the QGP should be formed also in elementary collisions like $p\bar{p}$ at a higher beam energy and the same energy density.

Further it is important to search for thresholds in the production of many particles e.g. Ω , which was found to be enhanced by a factor 15 above p+A data in Pb+Pb collisions at 158 A GeV [46] in the energy density region corresponding to the green stars in figure 7 (b). Similarly interesting would be a measurement of the invariant mass of e^+e^- in low energy densities.

6. Conclusions

In this letter, consequences resulting from the viable possibility that the dimuon invariant mass ($m(\mu^+\mu^-)$) enhancement, measured by the NA50 experiment in the intermediate mass region (IMR): $m(\phi) < m(\mu^+\mu^-) < m(J/\Psi)$, in S+U and Pb+Pb collisions at \sqrt{s} 19, 17 GeV, reflects a $D\bar{D}$ enhancement over expectations, are worked out.

The dependence of the J/Ψ and the $D\bar{D}$ yields per collision in Pb+Pb collisions on the mean number of participants has been estimated. This dependence reveals the non thermal features of charm production at this energy. The $\sim N^{0.7}$ dependence of the J/Ψ yield (figure 2) suggests strong dissociation of J/Ψ with higher centrality. The dissociation is stronger than the absorption seen in any other hadron, e.g. \bar{p} in Pb+Pb collisions. The N dependence of the $D\bar{D}$ yield of $N^{1.7}$ (figure 1) indicates also non-thermal open charm production at this energy, showing up in an excess rather than reduction as compared to the thermal expectation.

If the dimuon excess observed by NA50 is partly or solely due to open charm, it is appropriate to search for an anomalous suppression of J/Ψ as compared to the total open charm production, rather than to the DY process. We therefore investigated here the $(J/\Psi)/D\bar{D}$ ratio in Pb+Pb collisions and we find it to decrease approximately as $\sim N^{-1}$ (figures 3, 4). This is the N dependence expected for the J/Ψ if it were completely dissociated in quark gluon matter and were later dominantly formed through $c\bar{c}$ quark coalescence, assuming $N \sim$ volume of the $c\bar{c}$ environment and charm quark multiplicity of one in events with charm. In that case, based on coalescence arguments, the $(J/\Psi)/D\bar{D}$ ratio could be used

to estimate the volume of the charm environment, which may reflect partly the size of the quark gluon plasma. This is probable under the assumption that the final measured J/Ψ is dominated by the J/Ψ originating from $c\bar{c}$ pairs which travel through the plasma volume, an assumption which may hold only for large plasma volumes, i.e. for the most central collisions.

A further consequence of a possible open charm enhancement is that the J/Ψ over the $D\bar{D}$ ratio appears to be suppressed already in S+U collisions as compared to p+A collisions, unlike the $(J/\Psi)/DY$ ratio (figure 5). The $\psi'/D\bar{D}$ ratio would also be additionally suppressed as compared to the ψ'/DY in both S+U and Pb+Pb collisions. These phenomena could be interpreted as onset of dissociation of bound charm states above energy density $\epsilon \sim 1 \text{ GeV}/\text{fm}^3$.

We estimated and compared the dependence of the $(J/\Psi)/D\bar{D}$ ratio and of the kaon multiplicity per volume (assuming $K/N \sim K/V = \text{kaon number density}$) in several collisions and \sqrt{s} as a function of the initial energy density. We find that both the kaon number density and the ratio $(J/\Psi)/D\bar{D}$ exhibit dramatic changes at the energy density of $1 \text{ GeV}/\text{fm}^3$, as demonstrated in figure 7. This is the main result of this paper.

It follows that three major QGP signatures ($s\bar{s}$ enhancement, ρ changes and J/Ψ suppression) all appear above the energy density of $\sim 1 \text{ GeV}/\text{fm}^3$, which is the critical energy density for the QGP phase transition according to lattice QCD.

This discussion underlines the importance of a direct measurement of open charm production in nuclear collisions, and of other experimental investigations proposed in section 5, for the understanding of ultrarelativistic nuclear reactions and the dynamics of the Quark Gluon Plasma phase transition.

Acknowledgments

I would like to thank Prof. P. Minkowski, Prof. K. Pretzl, Prof. U. Heinz and Prof. J. Rafelski for stimulating discussions, and Dr. C. Cicalo, Dr. O. Drapier, Dr. C. Gerschel, Dr. E. Scomparin, Dr. P. Seyboth, Dr. F. Sikler, Dr. U. Wiedemann, and especially Dr. J.Y. Ollitrault for clarifying discussions on their data and/or for communicating their results to me.

REFERENCES

1. E. Laermann, Nucl. Phys. A 610 (1996) 1c.
2. T. Schäfer, Nucl. Phys. A610 (1996) 13c.
3. S. A. Bass et al., hep-ph/9810281, submitted to J. Phys. G, R. Stock, Nucl. Phys. A661 (1999) 282c, B. Müller, Nucl. Phys. A661 (1999) 272c.
4. T. Matsui, H. Satz, Phys. Lett. B 178 (1986) 416.
5. M.C. Abreu et al. (NA50 collaboration), CERN-EP-2000-013, Phys. Lett. B, in print.

6. M.C. Abreu et al. (NA50 collaboration), CERN-EP-2000-012, Eur. Phys. J. C, in print.
7. Z. Lin et al., Phys. Lett. B 444 (1998) 245.
8. C. Soave, Ph. D. Thesis, Universita Degli Studi Di Torino, Italy, April 1998.
9. R. Rapp and E. Shuryak, hep-ph/9909348, K. Gallmeister et al., hep-ph/9908269, P. Huovinen et al., Nucl. Phys. A650 (1999) 227.
10. P. Minkowski, private communication.
11. P. Minkowski, Phys. Lett. B 85 (1979) 231, F. Halzen et al, Phys. Rev. D27 (1983) 1631, S. Brodsky et al., Phys. Rev. D23 (1981) 2745.
12. M.C. Abreu et al. (NA50 collaboration), Phys. Lett. B450 (1999) 456.
13. C. Gerschel, private communication.
14. J.Y. Ollitrault, private communication.
15. J.P. Blaizot and J.Y. Ollitrault, Phys. Rev. Lett. 77 (1996) 170.
16. M. Gazdzicki, C. Markert, hep-ph/9904441, to appear in Acta Phys. Pol.
17. G. Ambrosini et al. (NA52 Collaboration), New J. of Phys. (1999) 1 22 (<http://www.iop.org>), CERN-OPEN-99-309.
18. C. Gerschel, Lectures given in Cracow School of Theoretical Physics, XXXIX Course, 1999, IPNO-DR 99-33.
19. F. Fleuret, Ph. D. Thesis, Ecole Polytechnique, France, LPNHE-X, 22 April 1997.
20. M.C. Abreu et al., (NA50 coll.), Phys. Lett. B 410 (1997) 337.
21. U. Heinz, U. Wiedemann, Phys. Rep. 319 (1999) 145-230, D. Ferenc et al., Phys. Lett. B 457 (1999) 347-352, U. Heinz, B. Jacak, Ann. Rev. Nucl. Sci. 49 (1999) 529.
22. E. Albini et al, Nucl. Phys. B 84 (1975) 269.
23. R. Ganz, (NA49 coll.), Nucl. Phys. A661 (1999) 448c.
24. U. Wiedemann, Nucl. Phys. A661 (1999) 65c.
25. J. Cleymans, K. Redlich, Phys. Rev. C 60 (1999), 054908.
26. E. Kolb, M. Turner, The early universe, Addison-Wesley publishing company, 1990.
27. R. A. Soltz, (E866 collaboration), Nucl. Phys. A661 (1999) 439c.
28. L. Ahle et al., (E802 and E866 collaborations), Phys. Rev. C 60 (1999) 044904, nucl-ex/9903009.
29. F. Sikler et al, (NA49 collaboration), Nucl. Phys. A661 (1999) 45c.
30. P. Seyboth, (NA49 collaboration), talk given in CERN Heavy Ion Forum, 26 July 1999.
31. E. Andersen et al., (WA97 collaboration), Phys. Lett. B 449 (1999) 401, CERN-EP-99-029.
32. J. D. Bjorken, Phys. Rev. D 27 (1983) 140.
33. P. Braun-Munzinger, J. Stachel, Nucl. Phys. A 638 (1998) 3, nucl-ex/9803015.
34. S. Margetis et al, (NA49 collaboration), Phys. Rev. Lett. 75 (1995) 3814.
35. J. Bächler et al, (NA35 collaboration), Z. Phys. C 51 (1991) 157.
36. K. Werner, Phys. Rep. 232 (1993) 87.
37. S. Kabana et al, (NA52 collaboration), J. of Phys. G, Vol. 25, Nr 2, (1999) 217.
38. S. Kabana et al, (NA52 collaboration), Nucl. Phys. A661 (1999) 370c.
39. P. Koch, B. Müller, J. Rafelski, Phys. Rep. 142 (1986), 167.
40. H. Satz, Nucl. Phys. A661 (1999) 104c.
41. B. Lenkeit et al. (CERES collaboration), Nucl. Phys. A661 (1999) 23c.

42. R. Rapp, Nucl. Phys. A661 (1999) 33c.
43. S. Kabana, P. Minkowski, Phys. Lett. B 472 (2000) 155, E-Print Archive: hep-ph/9907570.
44. C. Cicalo et al., Letter of Intent, CERN/SPSC 99-15; SPSC/I221; 7 May 1999.
45. J. Bartke et al., Z. Phys. C 48 (1990) 191.
46. E. Andersen et al., (WA97 collaboration), Phys. Lett. B 449 (1999) 401.

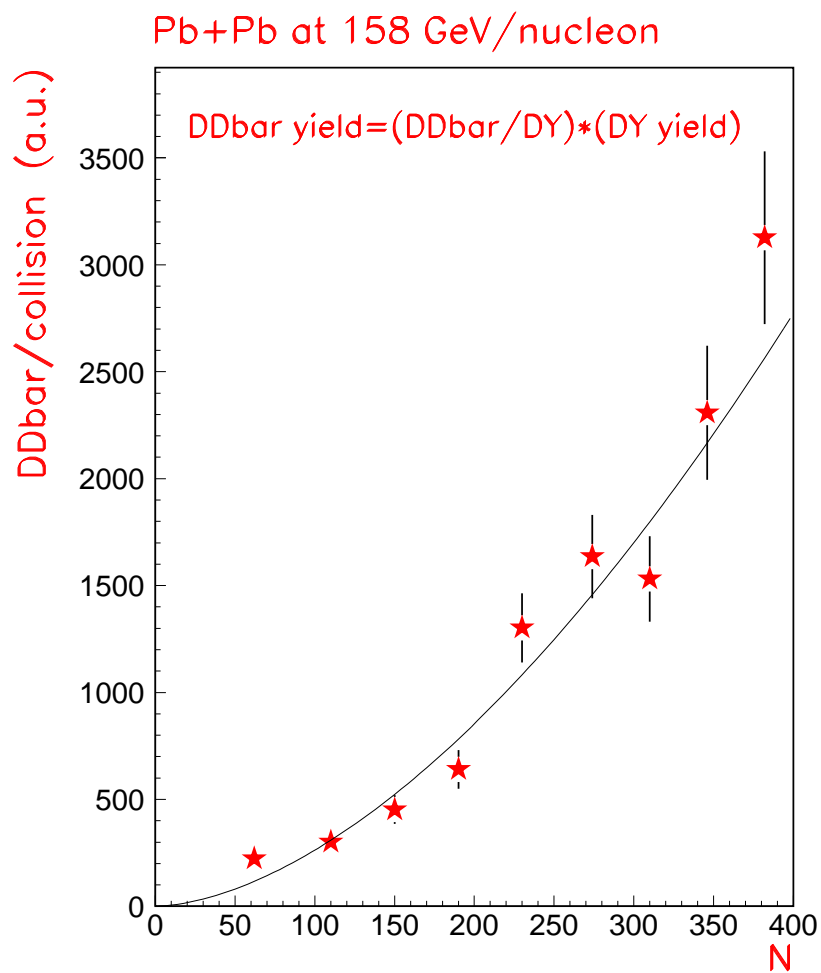


Figure 1. $D\bar{D}$ yield per collision in arbitrary units in Pb+Pb collisions at 158 A GeV, as a function of the number of participating nucleons N . The line shows the result of fitting the function $f = cN^\alpha$. See text for the fit results.

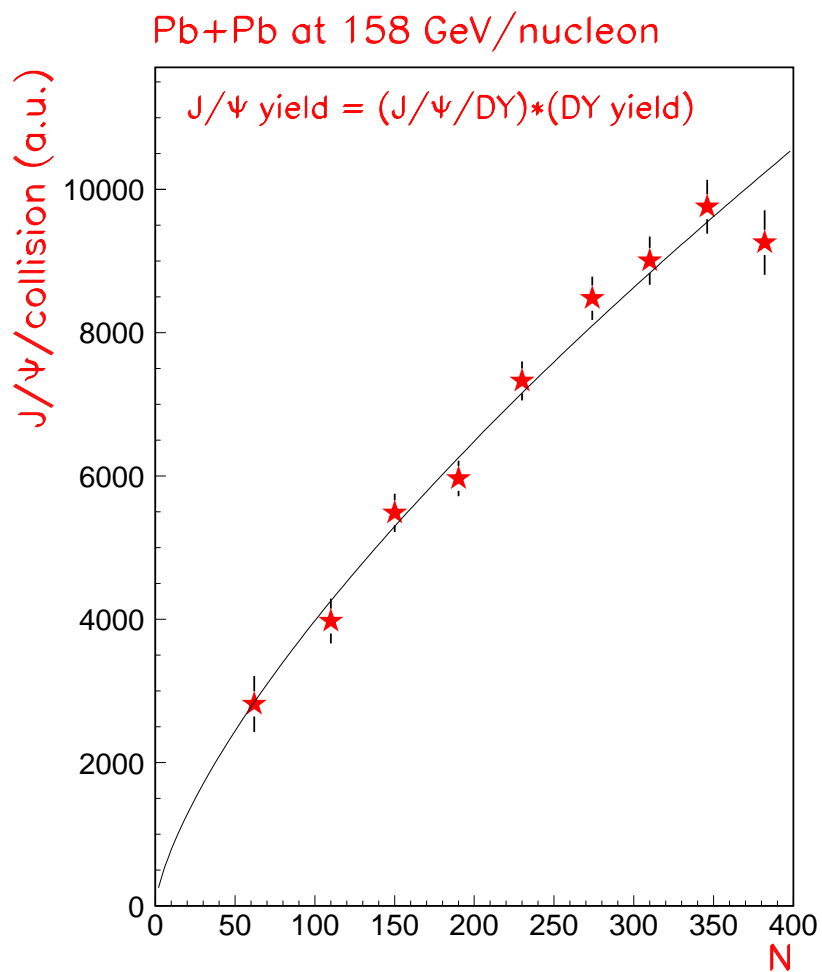


Figure 2. J/Ψ yield per collision in arbitrary units in Pb+Pb collisions at 158 A GeV, as a function of the number of participating nucleons N . The line shows the result of fitting the function $f = cN^\alpha$. See text for the fit results.

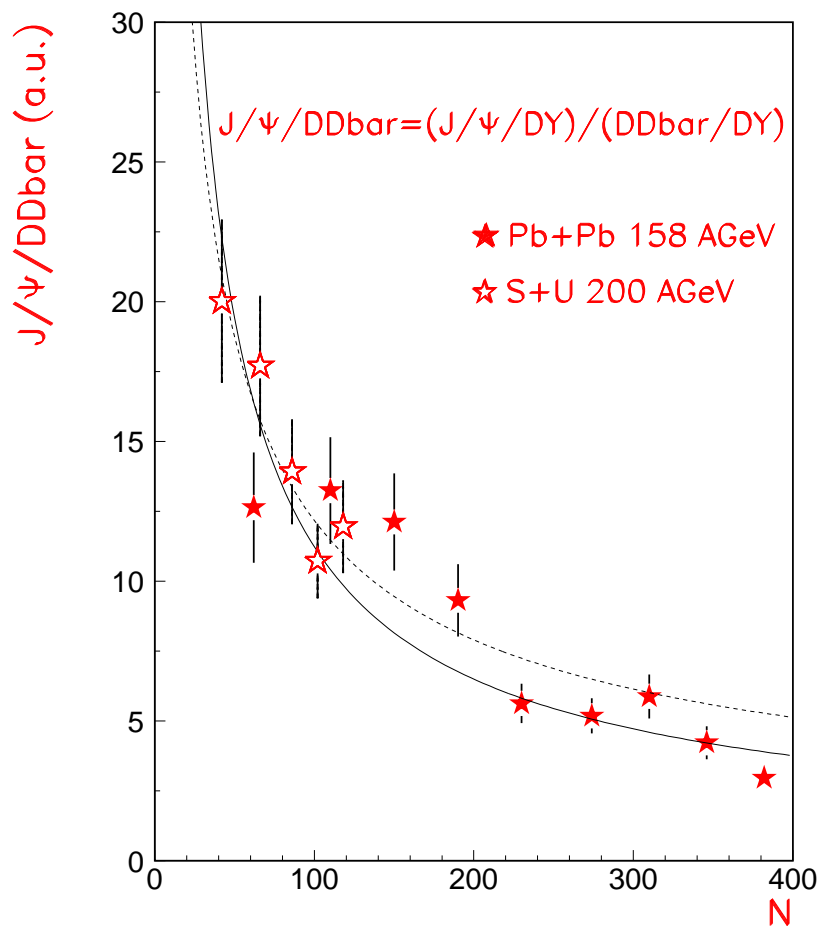


Figure 3. Ratio of J/Ψ to $DD\bar{D}$ in arbitrary units in Pb+Pb collisions at 158 A GeV (closed points) and in S+U collisions at 200 A GeV (open points), as a function of the number of participating nucleons N . The lines show the result of fitting the function $f = cN^\alpha$ to the S+U (line above) and to the Pb+Pb data points (line below). See text for the fit results.

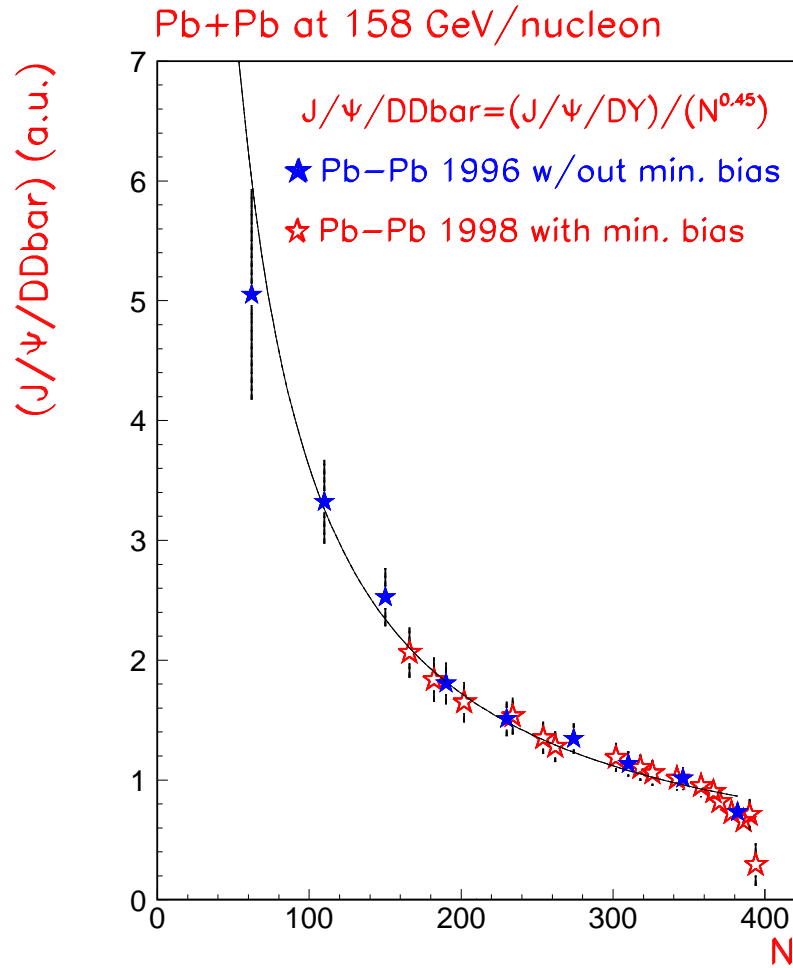


Figure 4. Ratio of $J/\psi/DY$ to $N^{0.45 \pm 0.11}$ in Pb+Pb collisions at 158 A GeV as a function of the number of participating nucleons N . The 9 closed star points correspond to the N values at which the $D\bar{D}$ yield was measured. The lines show the result of fitting the function $f = cN^\alpha$ to the closed stars. See text for the fit results.

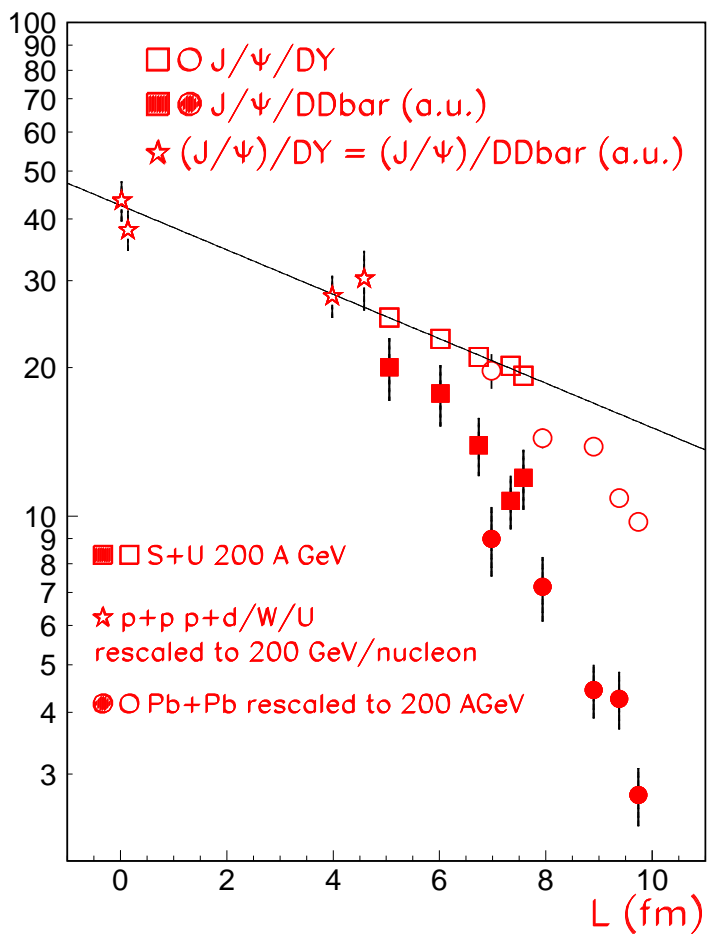


Figure 5. The open points show the ratio of J/ψ to Drell Yan (DY) in p+A, S+U and Pb+Pb collisions normalised to 200 A GeV, as a function of the path of J/ψ through nuclear matter L [20,19]. The closed points show the ratio of J/ψ to $D\bar{D}$ in S+U and Pb+Pb collisions at 200 A GeV estimated here. The open stars show the L dependence of the $J/\psi/DY$ and the $J/\psi/D\bar{D}$ ratio in p+A collisions. All $J/\psi/D\bar{D}$ ratios shown in this figure are in common arbitrary units.

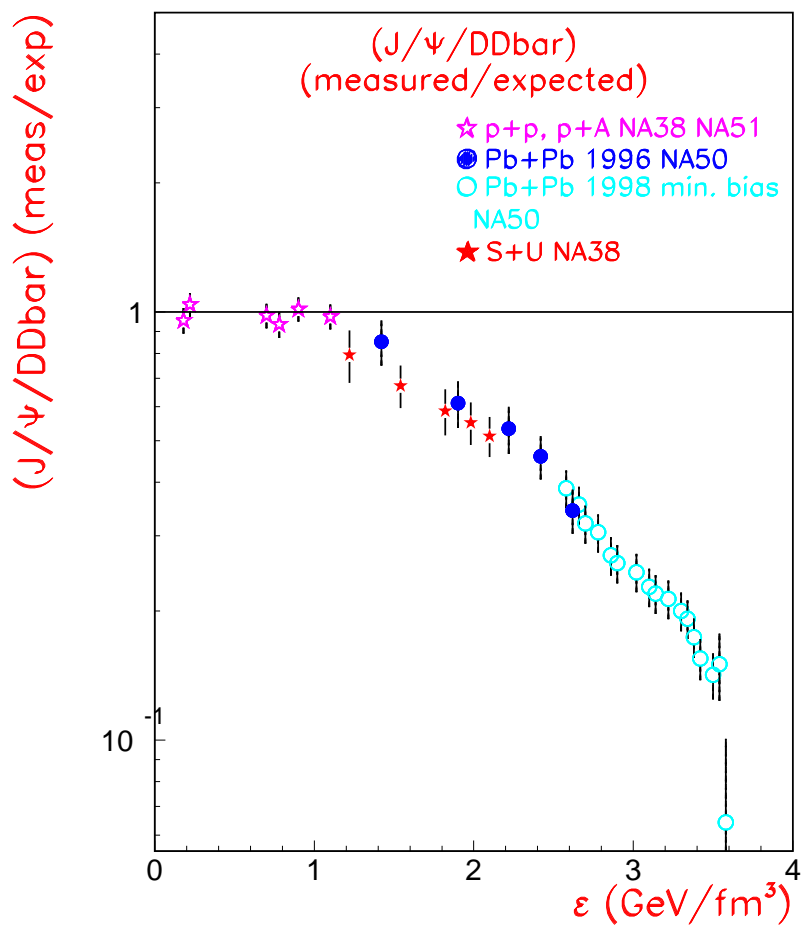


Figure 6. The $J/\Psi/DD\bar{D}$ (measured/'expected') ratio is shown as a function of the initial energy density (ϵ) achieved in the collisions investigated.

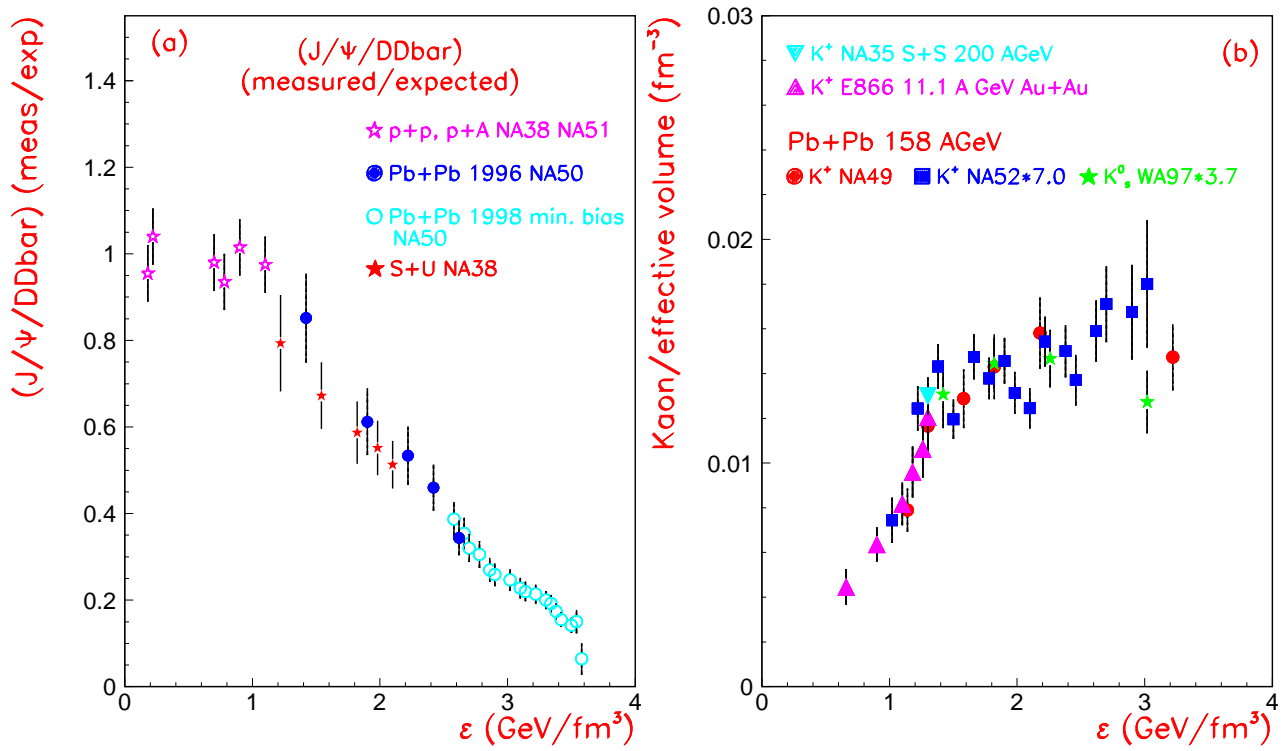


Figure 7. (a) The $J/\Psi/DD\bar{D}$ (measured/'expected') ratio is shown as a function of the initial energy density (ϵ) achieved in the collisions investigated. (b) The kaon ($\sim K^+$) multiplicity over the effective volume ($V = (\pi \cdot 4 \cdot R_{side}^2) \cdot (\sqrt{12} \cdot R_{long})$) of the particle source at thermal freeze out, in the center of mass frame, is shown as a function of the initial energy density (ϵ). The above effective volume is smaller than the real source volume but proportional to it.